Journal of Power Sources 196 (2011) 5264–5271

Contents lists available at ScienceDirect

Journal of Power Sources

journal homepage: www.elsevier.com/locate/jpowsour

Longevity test results for reformate polymer electrolyte membrane fuel cell stacks

J. Scholta[a,*], J. Pawlik[b], N. Chmielewski[c], L. Jörissen[a]

[a] Zentrum für Sonnenenergie- und Wasserstoff-Forschung Baden-Württemberg (ZSW), Helmholtzstr. 8, D-89081 Ulm, Germany
[b] Viessmann Werke GmbH & Co KG, Viessmannstr. 1, D-35108 Allendorf, Germany
[c] Proton Motor Fuel Cell GmbH, Benzstr. 7, D-82178 Puchheim, Germany

ARTICLE INFO

Article history:
Received 9 July 2010
Received in revised form 28 August 2010
Accepted 31 August 2010
Available online 15 September 2010

Keywords:
PEMFC
CHP
Longevity test
Long-term operation
Reformate operation
Degradation

ABSTRACT

Polymer electrolyte membrane fuel cell (PEMFC) stacks offer a great potential for combined heat and power (CHP) applications because of their good performance and technical maturity of the key components. Nonetheless, some developmental issues have remained open. Among those are the long-term stability with respect to performance degradation and sudden death phenomena like membrane rupture.

In a development program for domestic CHP systems, PEMFC stacks intended for long-term operation on reformate were developed. Development targets were high performance, high media utilization, good longevity and low degradation rates. In this paper, results on long-term performance tests of these stacks are reported. Operating times of more than 15,000 h with degradation rates of approx. 10 $\mu V\,h^{-1}$ have been achieved.

1. Introduction

The Viessmann Group is one of the leading international manufacturers of heating systems. Viessmann has developed field test units of a domestic cogeneration system based on a PEM fuel cell for detached and two-family houses. Natural gas is used as fuel for the system. ZSW has been working for more than 15 years in the field of polymer electrolyte membrane fuel cells (PEMFC), including the development of stacks from 2 W to 20 kW. Experimental results presented in this work are based on a PEMFC stack developed by Viessmann and ZSW. The developmental results with respect to stack technology are reported in [1,2].

Numerous data on PEMFC performance under ambient and pressurized conditions exists ([3–5]) but up to now only limited information on long-term performance tests are reported (e.g. [6–8]). Performance test results of PEMFC systems are given e.g. in [9]. The influence of contaminant gases (H_2S, NH_3, CO, ethylene) on the stack performance was reported in a previous publication [1].

Data shown in this publication are obtained using synthetic methane steam reformate including trace constituents such as CH_4, CO, and for certain test runs, air bleed.

The reported results were obtained using short and long stacks (10 and 60 cells, respectively). The cells have active areas of 148 cm^2 in the initial generation and 142 cm^2 in the improved generation. The stack improvement relates to the gas distribution fields, the membrane electrode assemblies (MEAs) and gas diffusion layers as well as operating conditions. Detailed results of the developmental activities are reported in [1,2]. Some aspects relevant for the flowfield and stack development are given in [10,11].

2. Experimental procedure

The long-term operation of PEMFC stacks was investigated using test benches with 24/7 capability which are described with respect to general layout in [3]. The anode and cathode gases were mixed using gas flow controllers (Millipore) which are controlled by a PLC unit (SIEMENS S7 300). Elektro-Automatik and Höcherl & Hackl electronic loads were used for the experiments. Both the anode and the cathode gases are humidified with bubbler humidifiers which temperatures are set according to Table 1 for the long-term operation tests. The standard reformate anode gas is a simulated reformate containing hydrogen with additional 30 mol% CO_2 and 5 mol% CH_4. CO and air bleed were added as specified below. The influence of gas compositions were investigated as close as possible to real operation conditions as the performance decay strongly depends on operating parameters such as cell temperature, gas composition, gas humidification and media utilization.

* Corresponding author. Tel.: +49 7319530206; fax: +49 7319530666.
E-mail address: joachim.scholta@zsw-bw.de (J. Scholta).

0378-7753/$ – see front matter © 2010 Elsevier B.V. All rights reserved.
doi:10.1016/j.jpowsour.2010.08.113

Table 1
Overview of selected stack endurance tests and corresponding operation conditions.

Stack no.	Number of cells	Operating hours (h)	MEA	Flow field	Active area (cm^2)	Media flow	Coolant inlet temperature (°C)	Utilization (%)		Dew point (°C)	
								Anode	Cathode	Anode	Cathode
1	10	2945	B	A	148	Counter	75	70	25	73	52
2	15	484	A	B_1	142	Counter	75	70	35–40	73	55
3	10	500	A	B	142	Counter	75	70	40	73	50
4	10	1700	A	B	142	Co	75	70	40	72	52
5	10	15000	B	B	142	Co	65	80	50	60	60
6	60	7000	B	B	142	Co	65	80	50	65	60

The cell temperature is kept according to levels specified in Table 1 operating temperature (coolant inlet) using the cooling water loop of the test bench. During the experiment, the cell was operated under current control. A predefined 24 h load cycle, which is shown in Fig. 1, was applied.

The load cycle included an OCV test under media flow. Every week, a current voltage curve and an OCV test under air shutdown were recorded. The settlement time was 15 min for each step of the current voltage curve (all data measured in a descending order) and 3 min for the OCV test without air supply.

This parameter field simulates the load changes expected for a CHP house energy supply. If some operating parameters could not be adjusted to the target values in the first phases of project, slightly modified parameters were used instead. The daily load changes (shown in Fig. 1) as well as the weekly characterization curves were integrated into the test bench program, such that the operation could be performed automatically. During the test phase, a semi automated analysis procedure was developed, such that curves like degradation over time, current voltage curves, OCV over time, and utilization voltage curves were generated with little operator interaction.

3. Results and discussion

3.1. Investigations on PEMFC stacks

The cumulated operation time of the stacks investigated was more than 65,000 h, which equals to an accumulated testing time of almost 8 years. The performance and long time behavior of stacks dependent on components selection and operating parameters were investigated.

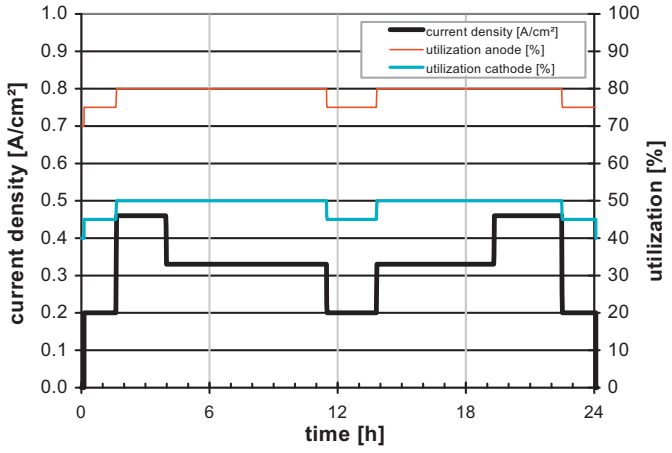

Fig. 1. Load cycle (one period) used for longevity tests (stack 5).

3.2. Long time performance tests of PEMFC stacks

The operation of the stacks was performed using a parameter field defined by Viessmann, which also includes time dependent load changes as given in Fig. 1. A summarizing table on all tests performed and the applied operating conditions are given in Table 1.

3.3. Initial long-term test results

The initial long-term test results, i.e. the results obtained with stacks prior to the improvements of the components and operating conditions, are reported in [1].

This status is represented by the test series of stack 1 (flowfield "A"). The operating time of stack 1 was 3000 h, using a standard reformate with 10 ppm CO. After that time, the media tightness was slightly reduced, presumably due to the beginning of pinhole formation. This reduction could be detected by anodic pressure drop tests showing a 90% pressure drop after 10 min waiting time with closed anode cell connectors. The degradation diagram is given in Fig. 2. The corresponding operating parameters (Table 1) also represent the range of possible operating points at that stage. It was possible to use anode utilization degrees of up to 75% and cathode utilization degrees of up to 35%. Two data points starting at 2500 h were recorded without CO, whereas all other data points were recorded with 10 ppm CO in the anode gas. A survey of current voltage curves is given in Fig. 3.

It can be concluded from current voltage curves given in Fig. 3, that most of the degradation effects are kinetic and active area reduction based. This analysis is supported by the degradation rates given in Fig. 2, which are comparably high for all current densities from 0.2 to 0.4 A cm^{-2} (24.6–29.7 μV h^{-1}), indicating that the main degradation process has a high effect already at current densities of ≤0.2 A cm^{-2}. On the other hand, OCV degradation rate under media flow is quite low (6.5 μV h^{-1}), such that only kinetic and active area reduction effects remain as possible mechanisms. Post test analysis of MEAs showed, that the electrodes were deactivated in some areas (visible as electrode material loss in some parts of the active area). This phenomenon overlapped with kinetic effects, and it is not possible to give exact figures on the contribution of both effects. For this stack, it is also difficult to distinguish between anodic and cathodic degradation processes, since the anode was operated almost permanently with CO containing gases, but it is expected from results reported below, that the observed degradation rates are caused both from anode and cathode degradation. At the end of operating time, also some mass transport limitations contribute to the voltage degradation. This can be concluded from the additional voltage decay of current voltage curves (shown in Fig. 3) from 0.5 to 0.6 A cm^{-2} at operating times of 2.000 h and more.

3.4. Long-term test results for the improved stacks

In a developmental program, which included simulations as well as experimental diagnostic techniques (area resolved current

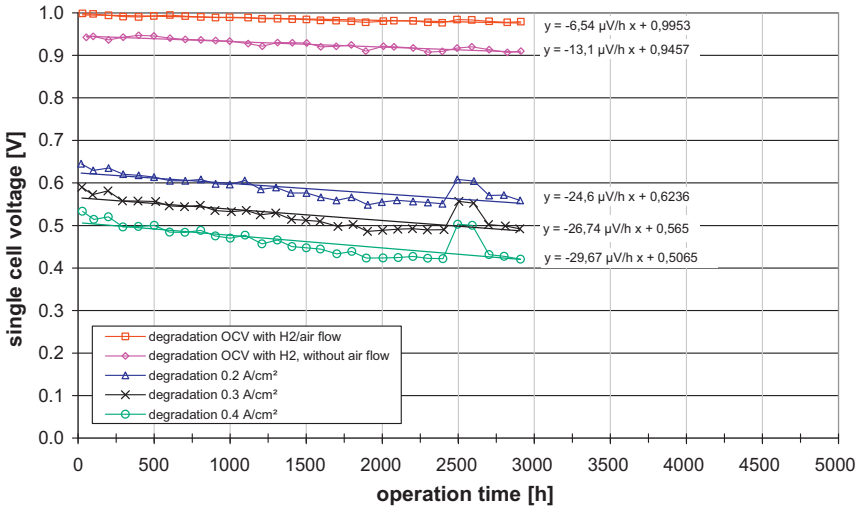

Fig. 2. Diagram of averaged single cell voltage vs. time for stack 1.

density measurements, flow simulations in transparent half cells, extended test programs with a wide range of operating conditions, including condensing operating parameters), the flow field geometry was changed both at the anode and the cathode side. The general approach was to reduce the parallelization degree of flowfield channels, including a reduction of the total cross sectional area of the flowfields. All relevant dimensions (rib and channel diameter, channel depth) were changed to less than 1 mm. The result of the flowfield improvements was a much better condensate removal capability even at ¼ of nominal media flow rates.

Also the GDL selection was optimized with respect to the new flowfield and the operating parameters selected. So, using the newly developed flow field type "B", it is possible to operate the stack routinely also under two phase conditions (formation of condensate within the stack). Utilization degrees of up to 80% (anode) and up to 50% (cathode) for a broad range of operating conditions have been achieved. The results are reported in detail in [1,2].

Due to the new MEA and improved flowfield and GDL, also the electrical efficiency and the degree of air utilization of the stack were improved. For some operating conditions, the air utilization was increased from 25 to 60% (stoichiometry 4–1.7). So, the use of flowfield B led to a big extension of allowable operating parameters. In Fig. 4 a comparison of operating points of both flowfield types is shown.

A more detailed analysis of the non stable operating points given in Fig. 4a was performed by measurements in a Perspex cell (flow velocity distribution), spatially resolved current density measurements, and by a theoretical analysis showed that there is a close interaction between expected or measured condensate formation, and a non stable cell performance. So, a better condensate removal capability was one of the main topics of flowfield development.

A set of corresponding current voltage curves is given in Fig. 5.

The current voltage curves show a decreasing voltage level with time, even within a short operation time. This is also shown in the voltage time characteristic of stack 2 (Fig. 6). The degradation rates are high and vary between 44 and 87 $\mu V\,h^{-1}$ under load. The test run of stack 2 and 3 were stopped after 500 h of operation out of the reason that the degradation rates were even higher compared to the initial stack (stack 1).

Combinations of further changes were necessary to reduce the degradation rates significantly. These changes include the operating parameters, especially the change from counter- to coflow (H_2/air), the reduction of the stack operating temperature, the selection of a more humid operation regime and an additional moderate anodic air bleed (0.8%). The influence of flow directions was investigated with stack 4, which was operated using the same conditions as for stack 3, but with coflow instead of counterflow. In

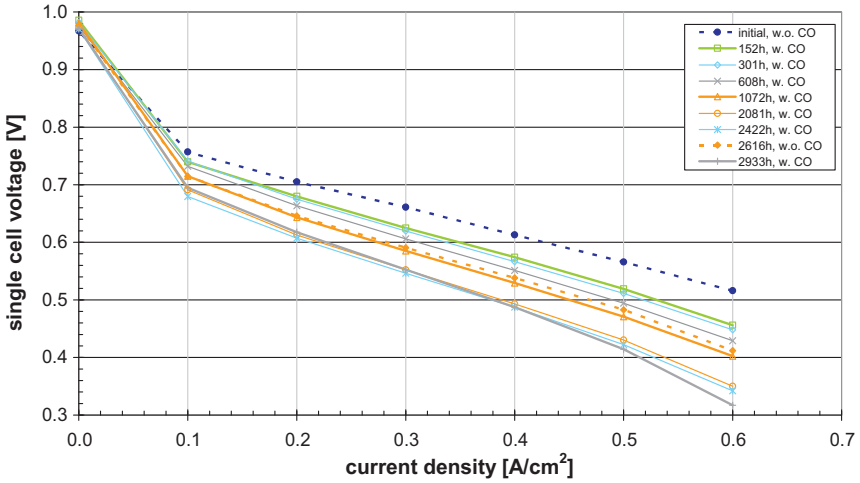

Fig. 3. Survey on current voltage curves for stack 1 (cathode utilization degree: 25%).

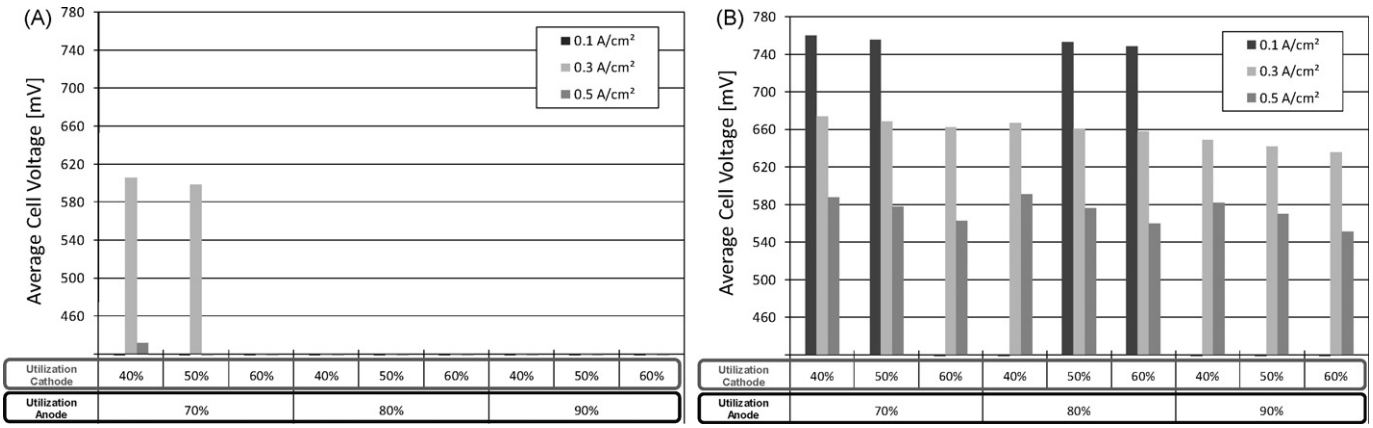

Fig. 4. Stable operating points and corresponding average cell voltages of a 5-cell stack for the reference cell design (flowfield A, a) and the improved cell design (flowfield B, b), reformate/air; ambient pressure at outlets; stack temperature: 75 °C; dewpoint anode/cathode: 75/30 °C.

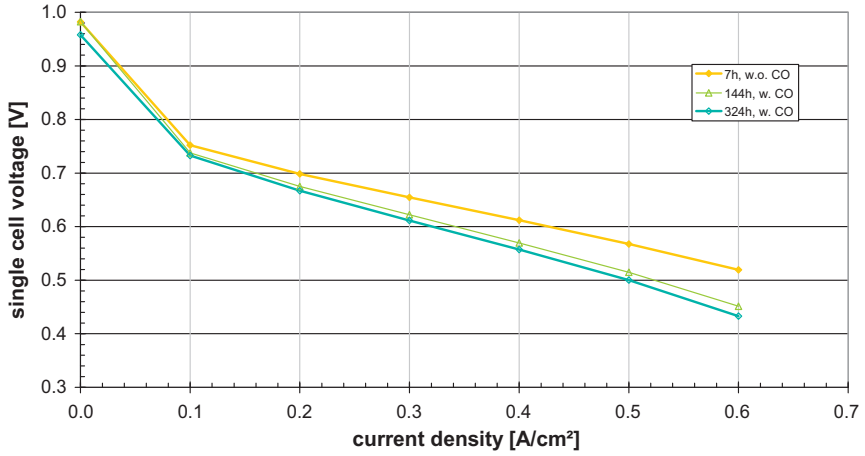

Fig. 5. Current voltage curves of stack 3 (cathode utilization: 40%).

Fig. 7, the corresponding voltage time diagram is shown. In Fig. 8, the current voltage curves of this stack are shown.

By the change to media coflow, the degradation rates were reduced from 44 to 82 $\mu V\,h^{-1}$ (stack 2) down to 21 to 36 $\mu V\,h^{-1}$ (stack 4). Also, the leakage rates (represented by OCV decay) were strongly reduced by the change from counter- to coflow. The corresponding values are 89 $\mu V\,h^{-1}$ for stack 2 but only 7 $\mu V\,h^{-1}$ for stack 4. The current voltage curves of stack 4 (Fig. 8) show no visible mass transport effects which might be due to less GDL hydrophobicity loss and less resulting flooding effects in stack 4 compared to stack 2.

In Fig. 9, the voltage time behavior for a 10-cell stack is given, and in Fig. 10 the voltage time chart for a 60-cell long stack is shown. Both stacks use the same materials and were operated nearly under

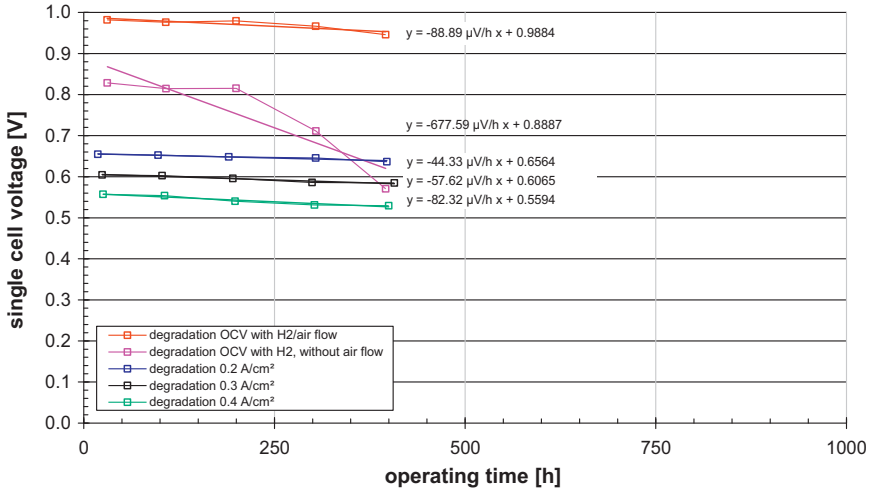

Fig. 6. Diagram of averaged single cell voltage vs. time of stack 2.

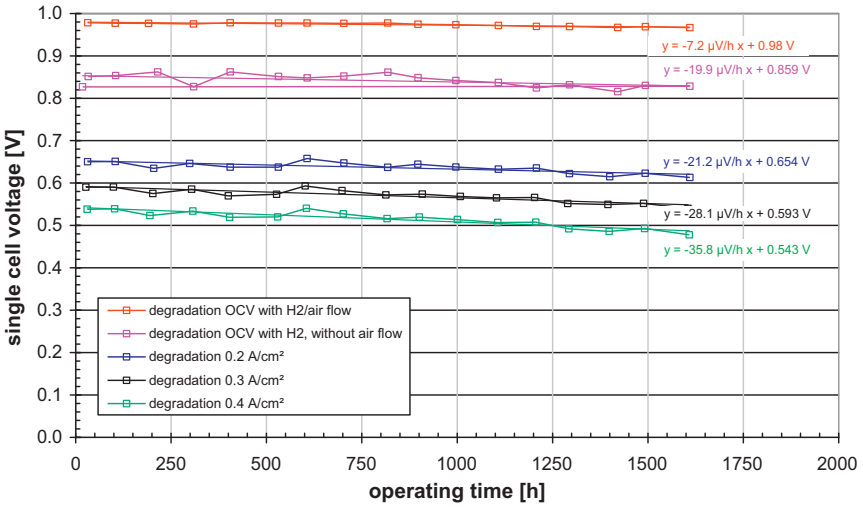

Fig. 7. Diagram of averaged single cell voltage vs. time of stack 4.

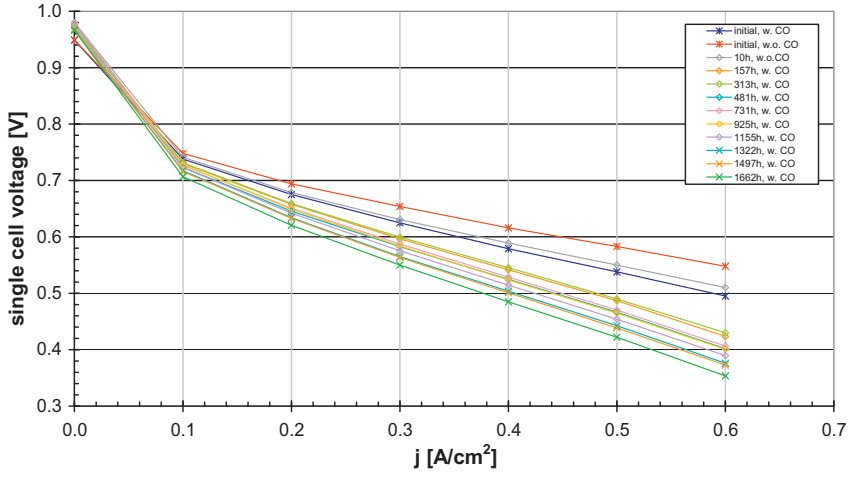

Fig. 8. Survey on current voltage curves of stack 4 (cathode utilization: 40%).

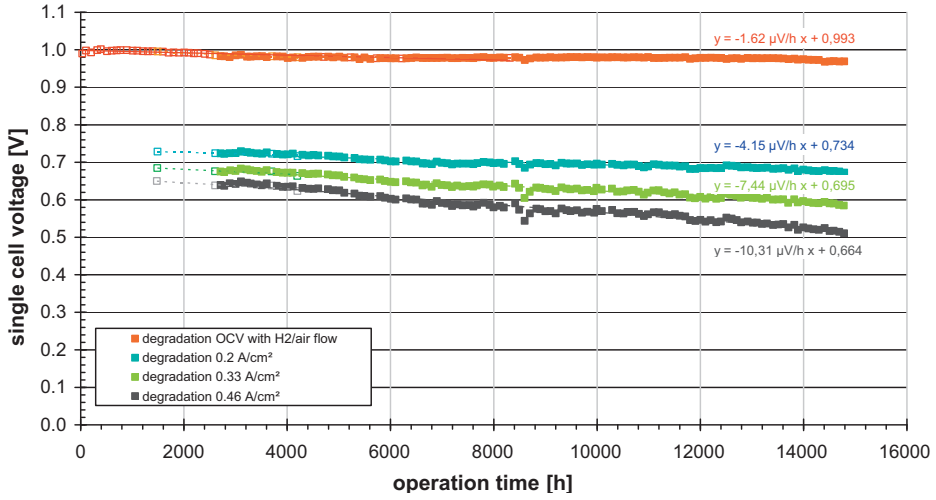

Fig. 9. Diagram of averaged single cell voltage vs. time of stack 5 (10 cells, cathode utilization: 50%).

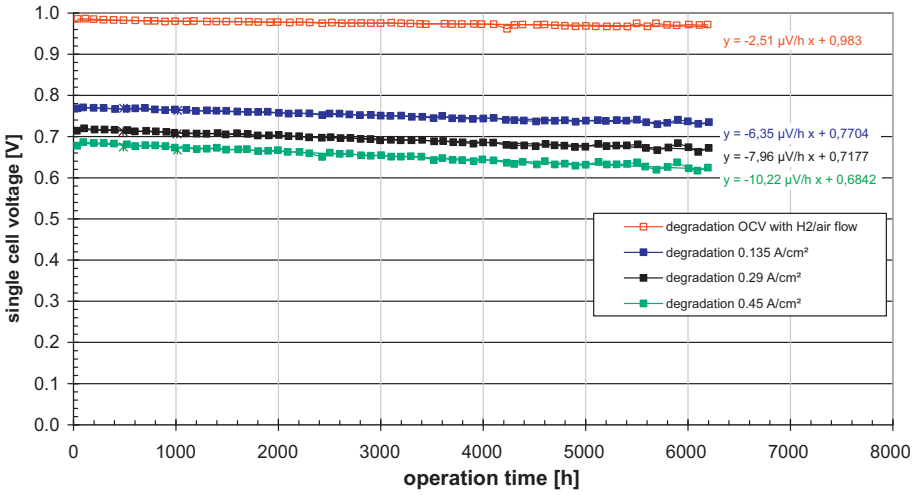

Fig. 10. Diagram of averaged single cell voltage vs. time of stack 6 (60 cells, cathode utilization: 50%).

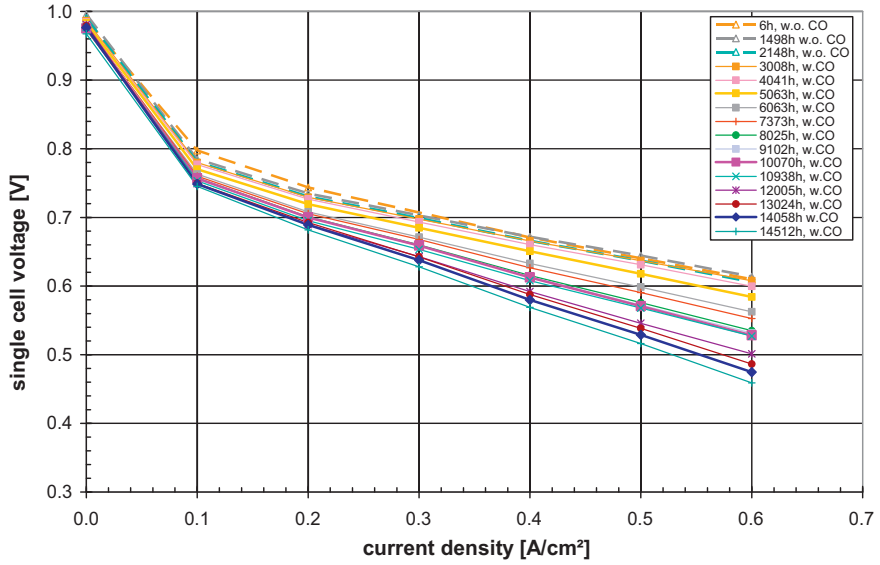

Fig. 11. Survey on current voltage curves of stack 5 (CO- and air bleed free and 10 ppm CO, 0.8% air bleed, air utilization: 45%).

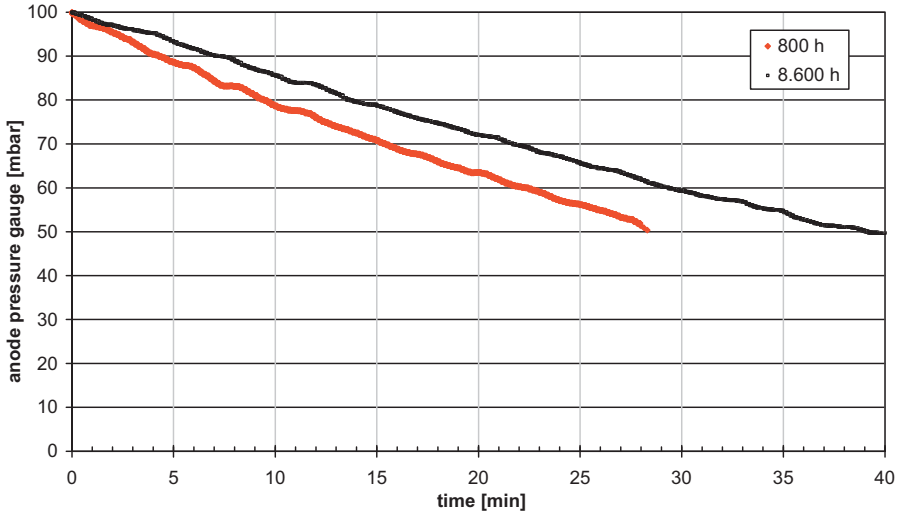

Fig. 12. Anodic pressure drop tests of stack 5 after start (800 h operation time), and after 8600 h operation time.

Table 2
Overview of selected stack endurance tests and corresponding voltage decay rates.

Stack no.	Number of cells	Operating hours (h)	MEA	Flow field	Active area (cm^2)	Media flow	Coolant inlet temperature (°C)	Voltage decay @ OCV ($\mu V\,h^{-1}$)	Voltage decay @ 0.2 A cm^{-2} ($\mu V\,h^{-1}$)	Voltage decay @ 0.3 A cm^{-2} ($\mu V\,h^{-1}$)	Voltage decay @ 0.4 A cm^{-2} ($\mu V\,h^{-1}$)
1	10	2945	B	A	148	Counter	75	6.5	24.6	26.7	29.7
2	15	484	A	B.1	142	Counter	75	88.9	44.3	57.6	82.3
3	10	500	A	B	142	Counter	75	112	–[a]	–[a]	–[a]
4	10	1700	A	B	142	Co	75	7.2	21.2	28.1	35.8
5	10	15000	B	B	142	Co	65	1.6	4.2	7.5	10.3
6	60	7000	B	B	142	Co	65	2.5	6.4	8.0	10.2

[a] No data available since change of operating conditions

the same conditions. The only difference is the number of cells per stack.

The operation time obtained was more than 15,000 h (10 cell) stacks, and more than 7000 h (60-cell long stack). The long stack test had to be terminated after that time for test bench failures, the 10-cell stack test is still ongoing. The degradation rates obtained (averaged data from 2300 to 15,000 h operating time) are ranging from 1.6 $\mu V\,h^{-1}$ (OCV with media flow) to 10.3 $\mu V\,h^{-1}$ (@0.46 A cm^{-2}). The long stack shows comparable degradation rates.

The corresponding current voltage curves for stack 5 (10-cell stack) are shown in Fig. 11.

The presented current voltage curves show only small and no increasing changes with time which are mainly contributed to kinetic effects. Moreover, it can be observed that small, but significant mass transport effects occur after more than 11,000 h operating time. The curves recorded with 10 ppm CO and 0.8 vol.% air bleed (starting after 2300 h operation time) show no significantly lower voltage levels than the curves recorded with CO- and air bleed-free reformate. This effect is independent of operation time; even after 10,000 h operating time there are no significant voltage changes, if both CO and air bleed are added. Other experiments reported in [12] show that the moderate air bleed dosage of 0.8% has even a protective effect with respect to a 10 ppm CO addition and related degradation effects. On the other hand, an additional performance decay can be observed, if CO is added and no air bleed is applied [1,13]. The OCV behavior under media flow (Fig. 9) indicates that no significant leakage formation occurs up to 15,000 h. The OCV line shows almost no degradation (approx. 1.6 $\mu V\,h^{-1}$) at all operation times. So it can be expected that the 10-cell stack can be operated for another several 1000 h. This assumption is also supported by gas leak tests which show no significant changes in anodic gas tightness from start to 8600 h (see Fig. 12). The pressure drop after 8600 h is even lower than close to initial stage. This variation lies in the measurement error.

4. Summary

The operation time obtained for a single stack could be increased from approx. 2500 h in the initial phase of the project to more than 15,000 h (ongoing test) in the ending phase. This more than a 6-fold increase is achieved by combined effects of stack development, material improvements, and a selection of operating parameters. The degradation rates were reduced from 50 to 80 $\mu V\,h^{-1}$ in the initial phase to 10.3 $\mu V\,h^{-1}$ (@0.46 A cm^{-2}) in the final phase. These achievements are accompanied by the change from H_2/N_2 mixtures to the use of simulated reformate (including 10 ppm CO and 0.8% air bleed). A survey on the degradation rates dependent on the operating conditions and stack type is given in Table 2.

It is shown that for the first stacks, the degradation rate is of similar amount for low and high current densities (stack 1) or may also be comparable for OCV and at high current densities (stack 2). The effect of a flow direction change can be observed comparing stacks 3 and 4, where almost no other change was made. These stacks were intentionally equipped with the more degradation sensitive membrane type “A”, to evaluate the influence of the cell design change on performance and degradation. The flow field change led to a higher degradation, if operated in counterflow mode (stacks 2 and 3), but the flow change to coflow allowed to reproduce the degradation rate obtained with the reference stack (stack 1), still obtaining a much broader window of operation parameters. A further reduction of degradation rate was obtained by a combined change of the MEA, maintaining the same base type of membrane, and a further change of operating parameters (stacks 5 and 6). In the optimized stacks (5 and 6), the degradation rates are very low at high current densities (approx. 10 $\mu V\,h^{-1}$), and are even smaller at lower current densities, such that a higher fraction of cell voltage level can be recovered by a slight current density reduction.

Moreover, the voltage level at a current density of 0.3 A cm^{-2} was increased from less than 600 mV to approximately 720 mV. At 0.5 A cm^{-2}, the corresponding voltage increase was from 560 mV for the initial stack to 660 mV in the improved stack (Figs. 2 and 10).

To achieve these results, long-term tests on more than 37 stacks with a total operating time of more than 65,000 h were performed.

5. Conclusions

The obtained results show a 6-fold increase of lifetime since start of the second project phase, combined with a voltage increase of 100 mV per cell at comparable operating points. The combined efforts of stack development, operation condition selection and materials development allowed to increase the operating time of stacks using reformate/air to more than 15,000 h with low degradation rates. This opens a perspective to achieve the operation targets for stationary operation in CHP units of 40,000 h under low degradation rates.

Acknowledgements

This project was funded by the German Federal Ministry of Economy and Trade under the project number 0327751A. The financial support is very much appreciated.

Literature

[1] J. Pawlik (Ed.), NG fuelled PEMFC house energy supply II (Ger), VDI Progress Report, vol. 576, VDI-Verlag, Düsseldorf, 2008.
[2] J. Pawlik, N. Chmielewski, J. Scholta, W. Lehnert, ECS Trans. 17 (1) (2008) 305–314.
[3] J. Scholta, N. Berg, P. Wilde, L. Jörissen, J. Garche, J. Power Sources 127 (2004) 206–211.
[4] J. Kolde, MEA Performance, FC Industry Report, vol. 4, no. 8, 2003.
[5] H.A. Gasteiger, et al., Handbook of Fuel Cells Performance, vol. 3, Wiley & Sons, 2003, pp. 593–610, ISBN 0-471-49926-9.
[6] S.D. Knights, K.M. Colbow, J. St-Pierre, D.P. Wilkinson, J. Power Sources 127 (2004) 127–134.

[7] Langlebige PEFC als Voraussetzung für eine Wasserstoffenergiewirtschaft, BMWi, FKZ 01SF0048, 2000–2005.
[8] B. Thoben, A. Siebke, J. New. Mat. Electrochem. Syst. 7 (2004) 13–20.
[9] M. Ferraro, F. Sergi, G. Brunaccini, G. Dispenza, L. Andaloro, V. Antonucci, J. Power Sources 193 (August) (2009) 342–348.
[10] J. Scholta, G. Escher, W. Zhang, L. Küppers, L. Jörissen, W. Lehnert, J. Power Sources 155 (1) (2006) 66–71.
[11] J. Scholta, F. Häußler, W. Zhang, L. Küppers, L. Jörissen, W. Lehnert, J. Power Sources 155 (1) (2006) 60–65.
[12] http://www.fctedi.eu/symposia/fqaspects/organizercontact/090910_4_LT_3_Scholta_Start_Stop.pdf, as of October 14th, 2009.
[13] A.A. Franco, M. Guinard, B. Barthe, O. Lemaire, Electrochim. Acta 54 (22) (2009) 5267–5279.